

Organic & Biomolecular Chemistry

Accepted Manuscript



This is an *Accepted Manuscript*, which has been through the Royal Society of Chemistry peer review process and has been accepted for publication.

Accepted Manuscripts are published online shortly after acceptance, before technical editing, formatting and proof reading. Using this free service, authors can make their results available to the community, in citable form, before we publish the edited article. We will replace this *Accepted Manuscript* with the edited and formatted *Advance Article* as soon as it is available.

You can find more information about *Accepted Manuscripts* in the [Information for Authors](#).

Please note that technical editing may introduce minor changes to the text and/or graphics, which may alter content. The journal's standard [Terms & Conditions](#) and the [Ethical guidelines](#) still apply. In no event shall the Royal Society of Chemistry be held responsible for any errors or omissions in this *Accepted Manuscript* or any consequences arising from the use of any information it contains.

ARTICLE

Fractional Transfer of a Free Unpaired Electron to Overcome Energy Barriers in the Formation of Fe⁴⁺ from Fe³⁺ during Core Contraction of Macrocycles: Implication for Heme Distortion

Cite this: DOI: 10.1039/x0xx00000x

Received 00th January 2012,
Accepted 00th January 2012

DOI: 10.1039/x0xx00000x

www.rsc.org/

Qihua Liu, Xiaochun Zhou, Haomin Liu, Xi Zhang, and Zaichun Zhou*

Abstract: The free unpaired electron in Fe³⁺ ions cannot be directly removed, and needs a transfer pathway with at least four steps to overcome the high energy barriers to form Fe⁴⁺ ions. Finer changes in the electronic structure of Fe³⁺ ions than spin conversion were identified through deeper analysis of the diffraction, spectral and electrochemical data for six nonplanar iron porphyrins. Fe³⁺ ions can form four d electron tautomers as the compression of the central ion is increased. This indicates that the Fe³⁺ ion undergoes a multistep electron transfer where the total energy gap of electron transfer is split into several smaller gaps to form high-valent Fe⁴⁺ ions. We find that the interchange of these four electron tautomers is clearly related to the core size of the macrocycle in the current series. The large energy barrier to produce iron(IV) complexes is overcome through a gradient effect of multiple energy levels. In addition, a possible porphyrin Fe³⁺ radical may be formed from its stable isoelectronic form, porphyrin Fe³⁺, under strong core contraction. These results indicate the important role of heme distortion in its catalytic oxidation functions.

Introduction

Iron porphyrins, including high-valent Fe⁴⁺ and Fe⁴⁺ π -cation radical species, show high reactivity in porphyrin catalytic systems,^{1,2} and are important reactive intermediates in various heme enzymes.^{3,4} Because of their oxidizing ability, porphyrin-related enzymes are capable of hydroxylating inactivated C–H bonds.⁵ Oxoiron(IV) porphyrin complexes are well investigated and relatively stable species in heme enzymes,^{6,7} but their formation and stabilization mechanisms are still unclear. It is more difficult to form iron(IV) species in planar macrocycles^{8,9} than in nonplanar ones.¹⁰ It was generally believed that the catalytic oxidation functions of heme mainly depended on structural changes in the macrocycle itself¹¹ and were regulated by the peripheral environment of the macrocycle.^{12,13} However, recent studies suggest that the conformation of the heme macrocycle may play a more important role in heme function

than the surrounding environment.^{14,15} The nonplanarity of the macrocycle in heme has been recognized as a structural feature that is conserved in specific proteins,¹⁶ and it induces specific properties including catalytic ability,¹⁷ tunable axial binding,¹⁸ large spectral red shifts,¹⁹ and adjustable rotation energy.²⁰ These observations suggest that nonplanarity is crucial to form high-valence iron(IV) species in porphyrins.²¹ However, few studies have directly focused on the relationship between the electronic and geometric structures of metalloporphyrins.^{10,22}

Recently, we systematically investigated the role of the nonplanarity (macrocyclic distortion) in heme and coenzyme B12 containing tetrapyrrole macrocycles using several series of strapped porphyrins or their complexes as models.^{23–25} We clarified (i) the relationship between macrocyclic distortion and core size,²³ and (ii) the effect of core size, which was controlled by macrocyclic distortion, on the electronic structure of the central metal ion, *e.g.*,

iron²⁴ and cobalt²⁵ (Figure 1). Early reports also demonstrated that the size of the porphyrin core can be changed by regulating the spin state of the iron(III)²⁶ and nickel(II)²⁷ ions within the highly deformed porphyrins.

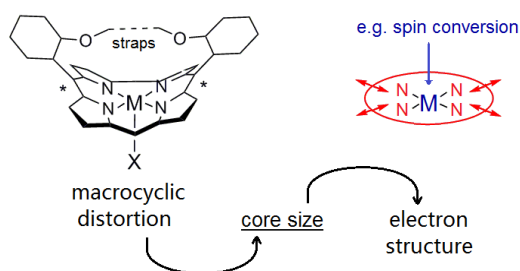


Figure 1. Change of core size controlled by macrocyclic distortion (left), and the electronic structure of central metal ions (M=Fe or Co) based on changes of core size (right). X represents a possible ligand such as Cl⁻ or MeOH.

These findings provided some indirect evidence of how a distorted macrocycle can not only stabilize the low-valent iron(II) oxidation state,²⁸ but also generate higher valence metallic complexes like iron(IV, V)²⁹ and cobalt(IV)^{30,31} by changing the core size alone. These results also implied that the actual role of the distortion in some protein enzymes³² is to regulate the electronic structure of central metal ions through contraction or expansion of the core. In current strapped models, the straps are used to regulate core size.

The sizes of metal ions with different charge and spin states are known (see supporting material S9).^{33,34} Changes in the structural and spectral trends of the model series can be conveniently attributed to the above relative states. Unfortunately, more detailed size parameters for these ions have not been obtained, and some weaker changes in the trends of iron porphyrin models have not been reasonably explained besides those arising from typical spin states.²⁴ We developed an interest in whether or not there are other states besides those with different charge and spin, and why a discontinuous change is observed in electron spin resonance (ESR) spectra of the model series.^{35,36} We also wished to understand why conformational isomers can form in the crystals of strapped iron porphyrins despite continuous contraction of the porphyrin core, and why different iron-containing species can coexist in heme.³⁷

In the current report, we demonstrate that the core contraction of porphyrins can result in more changes in the electronic structure of central Fe³⁺ ions than those outlined in our previous analysis.²⁴ The structure of the Fe³⁺ ion in the models undergoes further splitting besides the pure conversion between intermediate spin (IS) and low spin (LS) states when the central ion is compressed by core contraction. We also find that the splitting is based on a possible multistep electron transfer (et), which divides the total energy gap (Δ) of the electron transfer into several smaller fractional energy gaps (δ) before formation of a real Fe⁴⁺ ion (Figure 2). The large amount of energy needed to stabilize high-valent Fe⁴⁺ is perfectly decomposed through a possible energy gradient effect. These results indicate the vital role of the change in core size in the functions of iron porphyrins.

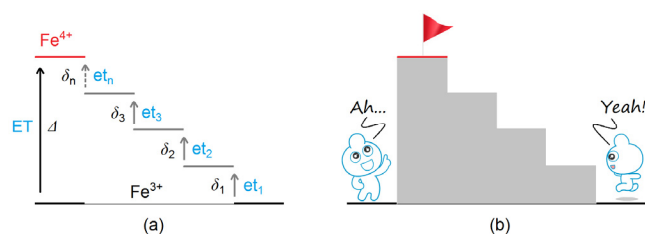
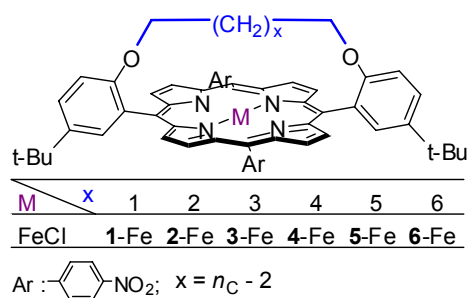


Figure 2. Comparison of (a) a model of the fractional transfer of an electron to form high-valent iron in heme with (b) stairs to facilitate climbing a slope. 'ET' and 'et' represent overall and fractional transfer, respectively, while ' Δ ' and ' δ ' are the total and fractional energy gaps between two ions, respectively.

Results and discussion

The series of 5,15-*meso-meso*-strapped iron(III) porphyrins **1-Fe** to **6-Fe** (Scheme 1) was selected as models for this study. In this work, we focus on the finer changes in the electronic structure of an Fe³⁺ ion than the conversion of spin states under core contraction. The crystal structure and ESR spectra of these models are reanalyzed to better understand the electronic structure of the central iron ion. The absorption spectra of these complexes cannot be used to differentiate these changes.³⁸



Scheme 1. Strapped iron porphyrins models **1-Fe** to **6-Fe**.

Detailed analysis of crystal results

Macrocyclic structure of porphyrins is of high flexibility. A slight variations of the macrocycle can induce marked changes in heme chemistry.³⁹ Computation result also showed that the saddle distortions is related to the prosperities of ferryl-porphyrin.⁴⁰ The crystal structures of iron(III) porphyrin models **1-Fe** to **6-Fe** revealed that the core size became consistently smaller as the straps were shortened, although there was some deviation originating from whether the number of carbon atoms in the straps was odd or even. One of the models, compound **3-Fe**, displays conformational isomers (Figure 3). In our previous work, these isomers were misidentified as twinning crystals because of the variable orientation of two *meso*-phenyl groups linked to the strap;²⁴ their small difference in core diameter is also readily obscured by the deviation resulting from whether the number of carbons in the strap was odd or even.

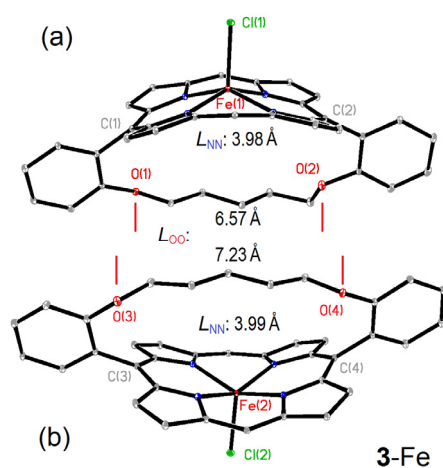


Figure 3. Conformational isomers of compound **3-Fe**.

Table 1. Pertinent structural parameters of the two isomers of compound **3-Fe**.

Parameter	3-Fe (a)	3-Fe (b)	ΔP_i^e
L_{NN} (Å) ^a	3.993	3.982	0.01
L_{OO} (Å) ^b	7.227	6.570	0.66
A_{NFeN} (°) ^c	151.8	151.0	0.8
A_{Cm} (°) ^d	22.6	24.2	1.6

^a L_{NN} is the core diameter represented by the average length of the diagonal N atoms in core units. ^b L_{OO} is the distance between two ether O atoms in the strap. ^c A_{NFeN} is the bond angle of the central iron atom and two diagonal N atoms. ^d A_{Cm} is the dihedral angle of 4 *meso*-carbon atoms. ^e ΔP_i is the absolute difference of each parameter of the two isomers.

Several structural features, however, demonstrate that the difference between the two isomers of **3-Fe** results from the change of the central ion rather than the macrocycle itself. Inspection of the crystal structure of the isomers of **3-Fe** shows that the slope orientation of two phenyl rings linked to the strap is the same, which implies that the frameworks in both isomers should be similar. However, this is not the case. Comparison of other structural parameters except for core diameter (L_{NN}) reveals their differences (Table 1). The distances between two ether O atoms (L_{OO}) in the strap in the two isomers are 7.23 and 6.57 Å; the difference between these values (0.66 Å), nearly half of a C-C bond length, is considerable. The differences in the bond angles of the central iron atom to two diagonal N atoms (A_{NFeN}) and dihedral angles of four *meso*-carbon atoms (A_{Cm}) of the two isomers are also substantial at 0.8° and 1.6°, respectively. These differences suggest that the formation of the isomers of **3-Fe** originates from the isoelectronic structure of the central iron(III) ion.

The existence of conformational isomers of **3-Fe** indicates the presence and stability of electron tautomers in d orbitals of the Fe^{3+} ion. In other words, the two isomers result from two of the electron

tautomers of the iron(III) ion. The formation of conformational isomers is the macroscopic expression of microscopic electron tautomerization in the central metal ions. The IS Fe^{3+} ion (defined as relative high-spin in our previous report)²⁴ really includes two subforms, which we term IS_a and IS_b .

The macrocycle core diameter can be divided into three sections, two in the IS field, and one in the LS field (Figure 4). The two stages in the IS field are attributed to the two subforms IS_a and IS_b , while that in the LS field is attributed to subform LS_a . The solid structures of the existing models include these three electronic structures of Fe^{3+} ions.

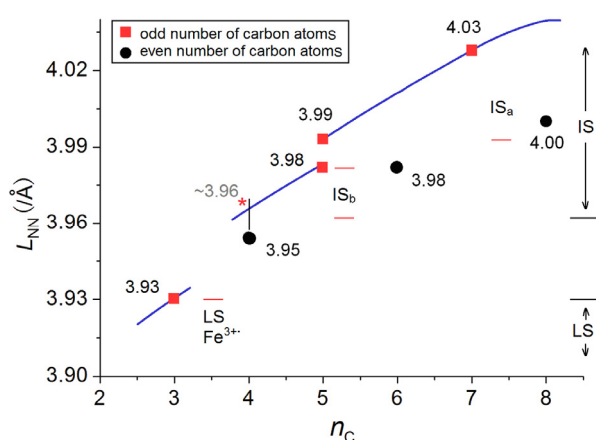


Figure 4. Relationship between the subforms of electronic structure in Fe^{3+} ions and the core size of the macrocycle.

The size contraction was originally interpreted as two independent trends depending on whether there was an odd or even number of carbon atoms in the strap. This is because an even number of carbon atoms induces macrocycle distortion with more irregular features than an odd number. As a result, only one series of core diameter parameters (L_{NN}) of the compounds with an odd number of carbon atoms in the straps were used to evaluate the change of electronic structure in the central metal ions in the current analysis. The purpose of this is to eliminate the disturbance from irregular deformation caused by the fluctuation between odd and even numbers of carbon atoms. (See supporting material S2-S5.)

Note that the formation of conformational isomers in iron porphyrin models is not an isolated case; this phenomenon can be

found in each series of model porphyrin complexes containing the metal ions magnesium(III), cobalt(II) and nickel(II). (See supporting material S6-S8.)

Finer analysis of ESR spectral results

The macrocyclic deformation of porphyrin has a considerable influence on the spin state of the central iron(III) ion.^{26,35,41} For the current iron porphyrin series, the ESR results can also be divided into two categories: an IS section containing the five samples from **6-Fe** to **2-Fe**, and a LS one containing just **1-Fe**. Spin conversion of Fe^{3+} ions from IS to LS forms occurs between the two sections (Figure 5). A detailed assignment of ESR spectral results to spin modes was presented in our previous report.²⁴ ESR measurements of toluene solutions of **1-Fe** to **6-Fe** were performed under inert gas at a concentration of ~ 3.0 mol/L. Spectra were recorded at 130 K with a microwave power of 998 μW at 9.0408 GHz, modulation amplitude of 0.25 mT, and modulation frequency of 100 kHz. Below we reanalyze these ESR results considering the IS and LS categories.

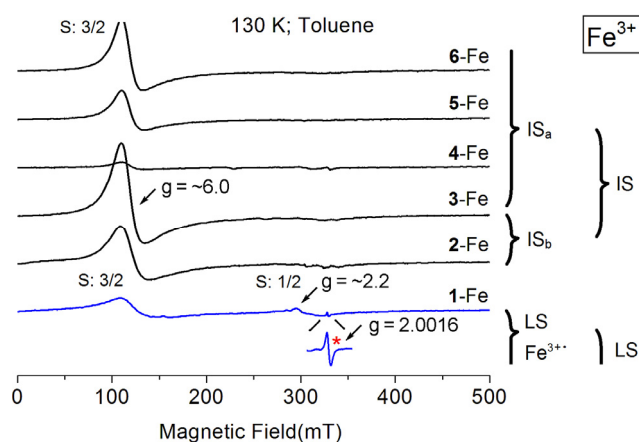


Figure 5. ESR spectra of solid samples of the model iron porphyrins **1-Fe** to **6-Fe**. The ESR data are from our last report.²⁴ 'IS' and 'LS' represent intermediate- and low-spin states, respectively. The red asterisk denotes the radical.

In the ESR spectra of IS materials **6-Fe** to **2-Fe**, their paramagnetic intensity ($g \sim 6.0$) exhibits two periodic trends, rather

than a continuous one like that of core contraction. Two relatively intense signals are found in the ESR spectra of compound **6-Fe** and **3-Fe**. The signal intensity of these two compounds became progressively weaker as the core contracted, which is observed as two periods. The ESR spectrum of the LS compound **1-Fe** implies that the Fe species is a mixture of IS_b Fe^{3+} , LS Fe^{3+} and a possible Fe^{3+} radical. The radical signal (indicated by an asterisk in Figure 5) can be attributed to the delocalization of an active electron. The iron porphyrin **3-Fe** radical, an electron tautomer of porphyrin **3-Fe**, is believed to be capable of catalyzing oxygenation and oxidation reactions.³

An energy ladder model with small gaps between each level can be established based on the comprehensive results of the changes in core size and electron forms in spin states (Figure 6). According to the heights of the energy levels of all of the subforms, the Fe^{3+} ion can form four electron tautomers, IS_a , IS_b , LS_a and Fe^{3+} in the isoporphyrins before elimination of a valence electron from the tautomers of the Fe^{3+} ion. From the perspective of energy levels, the fractional energy gap (δ) between adjacent tautomers is believed to become much smaller than the total energy gap (Δ) between typical Fe^{3+} and Fe^{4+} ions. The size range of the core diameter of each subform for the current series is shown in Figure 6. The typical Fe^{3+} ion is not capable of catalyzing oxygenation and oxidation reactions, whereas the Fe^{3+} radical is. It is thought that the interchanges of these isoporphyrins are only related to core size in these models, which reveals the importance of core contraction.

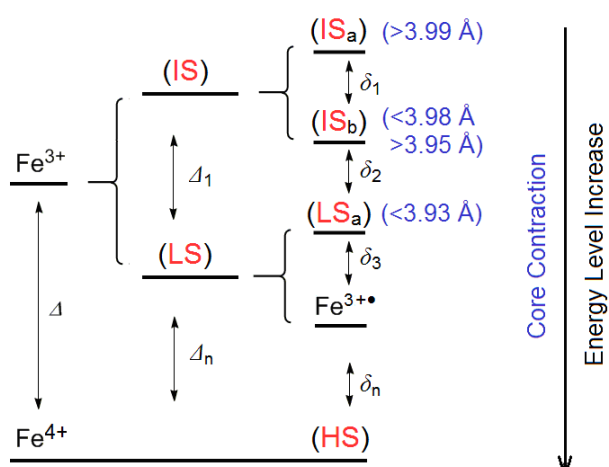


Figure 6. Energy ladder model representing the relative molecular energy level of each subform under core contraction. The core diameter range of each of subform in the current series is shown in blue. The symbols ' Δ ' and ' δ ' are as described in Figure 2.

This energy ladder model explains why conformational isomers can coexist in compound **3-Fe**, and why this phenomenon occurs only once in this series of complexes. Thus, adjacent electron tautomers with different charge number and spin mode may readily interchange when their energy gap (δ) is decreased sufficiently by slightly adjusting core size, making the coexistence of these subforms possible. In other words, the formation of conformational isomers can take place between any two adjacent subforms only when the core size is suitable.

Model of fractional transfer of an electron in iron ions

We then examined the electronic structure of each subform. Corresponding to the above energy ladder model for Fe^{3+} ions, a fractional et model was devised, as shown in Figure 7. This model can clearly track the electron movement in Fe^{3+} ions during core contraction.⁴²

In the IS section ($S=3/2$), it was thought that the 4-N unit effectively maintained the normal dsp^2 coordination mode (IS_a) in compounds **6-Fe** to **4-Fe** and completely changed to the inner form (IS_b) in samples **3-Fe** to **2-Fe**.^{43,44} The unpaired electron in the $3d_z^2$ orbital jumps to a higher $3d_{x^2-y^2}$ orbital in latter two compounds because their core cavity is still large enough to accommodate the behavior of the single electron; that is, the unpaired electron and an electron pair in the 4-N unit exchange their positions between IS_a and IS_b (S_1 exchange). Interchange between these two states could happen under suitable conditions, which is when the two subforms have a similar core size and close energy levels. The structural parameters (e.g., $\Delta L_{NN}=0.01 \text{ \AA}$) of the two isomers in **3-Fe** (Figure 3) show that the size condition can be met, and the coexistence of the isomers further indicates their energy levels are similar.

The electron rearrangement of two subforms can also explain the periodicity in the ESR intensity of the series (Figure 5). In the model series, the iron ions are confined by the porphyrin, which prevents external molecules from disturbing their electronic structure. Relative ESR intensity mainly depends on the degree of magnetic coupling among single electrons.^{45,46} In the IS_a state, the weakening of paramagnetic intensity originates from the strengthening of the attraction of three single electrons because of their internal magnetic decoupling as the metal ion radius decreases from compound 6-Fe to 4-Fe. In state IS_b , the strong ESR signal mainly derived from the free unpaired electron will be weakened as the radius decreases from 3-Fe to 2-Fe; the paramagnetic weakening is for the same reason as that in the IS_a stage. Thus electron exchange actually activates the unpaired electron in the $3d_z^2$ orbital.

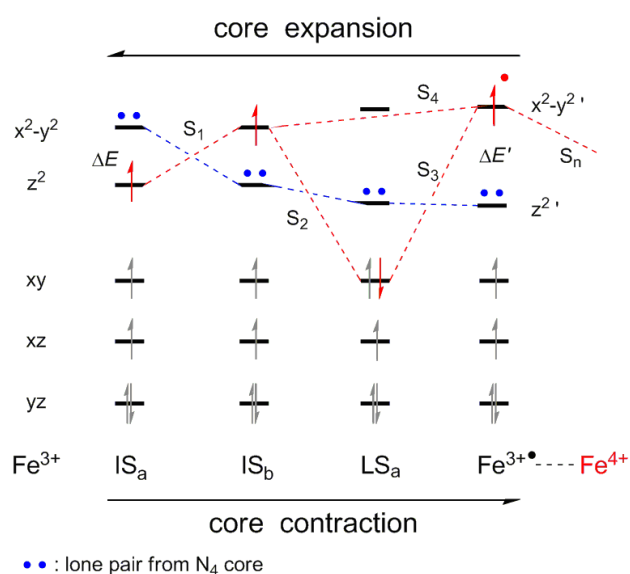


Figure 7. Electronic fractional transfer model showing the real electronic behavior of Fe³⁺ ions as the core contracts. 'S' represents electron behavior, S₁: exchange, S₂: transition 1, S₃: transition 2, S₄: migration. '•' indicates the delocalized electron.

Ideally, the unpaired electron in the $3d_{x^2-y^2}$ orbital will be either transferred to a 3d orbital (e.g., $3d_{xy}$) of lower energy, or stabilize the current orbital as the core is fully reduced. Both steps are labeled as S₂ (transition 1) and S₄ (migration). The former step occurs as expected. The unpaired electron in the $4d_{x^2-y^2}$ orbital is eventually removed and is preferentially paired in a lower energy 3d orbital as

the core shrinks (S₂ electron transition 1), producing a new subform (LS_a). The electronic structure of the Fe³⁺ ion is converted to LS (S=1/2), which is evidenced by a g-value of 2.2 in the EPR measurements. 1-Fe in the solid state should mainly be composed of this subform.

However, the latter step does not occur as expected.⁴⁷ The ESR data for compound 1-Fe reveal the coexistence of IS Fe³⁺ and a possible Fe³⁺ radical, rather than IS Fe³⁺ alone. Macrocyclic deformation, which can determine the metallic spin state in ruffled porphyrins, can also influence field strength by changing the energy level splitting of 3d orbitals.^{48,49} It was thought that the energy level of the $3d_{x^2-y^2}$ orbital would increase and the unpaired electron would migrate to the new $3d_{x^2-y^2}$ orbital (S₄ migration) because of larger splitting between the $3d_z^2$ and $3d_{x^2-y^2}$ orbitals as the core is fully contracted. The unpaired electron in the new orbital may partially tend to delocalize over the large π system to produce an active electron (shown as a radical) to some degree. It is unknown whether the radical electron in the Fe³⁺ state is from LS_a (S₃ transition 2) because there is no evidence for this. Fortunately, this does not prevent us from differentiating the three subforms IS_b, LS_a and Fe³⁺ according to core size. It is expected that the ratio of the Fe³⁺ state would be enhanced in a mixture coexisting with the LS_a form under stronger contraction. Coexistence of two adjacent spin states has been confirmed for deformed iron porphyrins, which can produce spin-crossover complexes using the Mössbauer technique.³⁸

The fractional et model can clearly explain the stability and coexistence of the electron tautomers of the Fe³⁺ ion. The most important factor is that the gap (δ) between energy levels becomes small enough to allow electron movement between adjacent subforms for a specific core size, which maintains the coexistence of the electron tautomers, IS_a, IS_b, LS_a and a Fe³⁺ radical of the Fe³⁺ ion. This electron movement does not occur spontaneously for other core sizes, which maintains the stability of each subform.

The fractional transfer model can also readily explain the role of ligand participants in the catalytic systems of porphyrins containing iron, e.g., triphenylphosphine and pyridine in catalytic oxidation of iron porphyrins,⁵⁰ and imidazolyl⁵¹ and sulfhydryl⁵² moieties in the

residue groups of amino acids as ligands in heme enzymes. For example, the ligand participant will be very important if it influences the IS_b state. Such ligands can both increase the radii of metal ions to meet the required core size, and drive transfer of a valence electron to convert between two subforms, IS_b and LS_a . At the same time, the ligand participant has a recycling function of ligation and deligation because of the exchange of the valence electron between $3d_z^2$ and $3d_{x^2-y^2}$ orbitals during contraction. This principle is supported by the fact that the coordination number of iron ions in heme changes between 5 and 6.²²

Electrochemical analysis of metalloporphyrins

The nonplanarity of porphyrin can slightly affect the shift in redox potential of metalloporphyrins because of changes of electron density.⁵³ Cyclic voltammograms of the model compounds were measured at room temperature in solutions of benzonitrile and 0.2 M tetra-*n*-butylammonium hexafluorophosphate (TBAH) at a scan rate of 0.1 V/s, and are depicted in Figure 8.

The potentials for the Fe(IV)/Fe(III) reaction shift to more negative value from 1.29 to 1.19 V (Figure 8, indicated by filled circles) based on the increased degree of distortion in the macrocycle from 6-Fe to 1-Fe. The potentials for Fe(III)/Fe(II) at low voltage show a similar trend as the degree of distortion increased (indicated by squares); the peak voltage (E_p) shifted from -0.25 to -0.50 V. This shift to more negative value can be interpreted as an increase of the electron density on the central metal ion during core contraction.^{54,55} Such shifts have also been found for other nonplanar porphyrin systems, and were derived from not only the metal ion, such as nickel or copper,⁵⁶ but also the deformed macrocycle itself.⁵⁷ These electrochemical results are similar to those obtained for regular iron porphyrins.⁵⁸

For 4-Fe, 3-Fe and 2-Fe, E_p of the Fe(IV)/Fe(III) reaction splits and forms a new peak in the range of 0.89 to 0.99 V (Figure 8, labeled as empty circles). For convenience, the split potential signals of the reaction are defined as the second reduction (named IV/III_b) of the Fe(IV)/Fe(III) couple. The original signals at 1.19 to 1.29 V are

defined as the first reduction (IV/III_a) of this couple. The second reduction is shifted to more negative value by up to 0.26 V from the first reduction. This negative shift is not observed for compounds 6-Fe and 5-Fe with lower degrees of distortion and 1-Fe with higher.

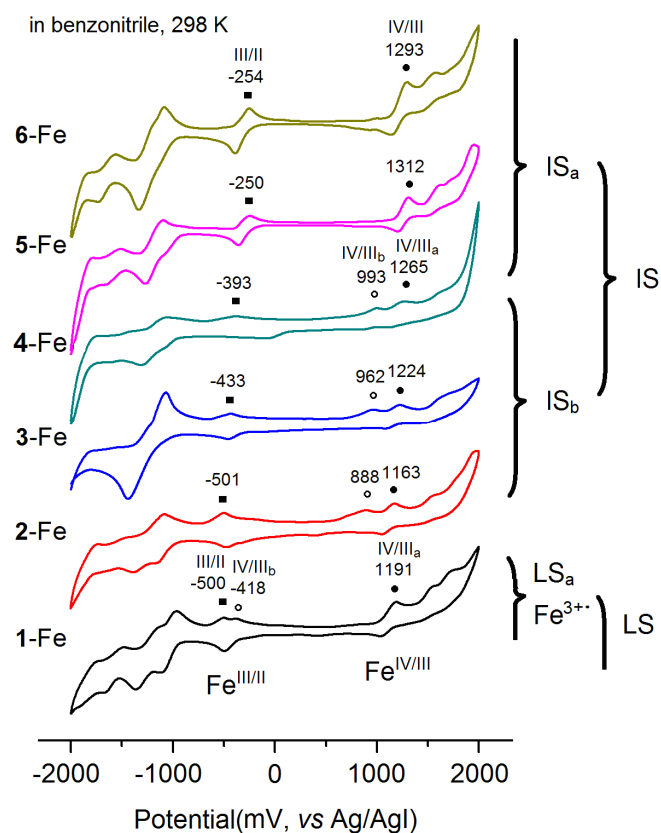


Figure 8. Cyclic voltammograms measured for the iron porphyrin series.

The signal splitting of the Fe(IV)/Fe(III) reaction is derived from the formation of conformational isomers in the complex of 3-Fe (Figure 3). The first and second reduction peaks, IV/III_a and IV/III_b, of the Fe(IV)/Fe(III) couple correspond to the two electron tautomers IS_a and IS_b of the Fe^{3+} ion, respectively (Figure 5). The conformational isomers of the model 3-Fe and ESR spectra for the six complexes support the above relationship. In the IS_b state of Fe^{3+} , the unpaired electron is found in the $3d_{x^2-y^2}$ orbital with a higher energy level than the $3d_z^2$ orbital in the IS_a state because of core compression, which makes the potential of the IS_b state lower than that of the IS_a state.

According to the crystal structures of the models, the splitting of the Fe(IV)/Fe(III) reaction can only occur in **3-Fe**, and not in **4-Fe** and **2-Fe** because these complexes do not have isomers. It is believed that thermal movement and ligation/deligation of benzonitrile causes splitting of the Fe(IV)/Fe(III) reaction. A report showed that the electrochemistry of iron porphyrins could be fine-tuned by axial ligands like pyridine.⁵⁹ In this study, benzonitrile acted as both solvent and axial ligand, finely tuning the electron density of the central iron ion. As a result, the two compounds adjacent to **3-Fe**, **4-Fe** and **2-Fe**, can also isomerize in benzonitrile.

The electrochemical results for complex **1-Fe** reveal that its second reduction peak at -0.42 V appears at a quite different position from those for **2-Fe** to **4-Fe**. The peak is close to the potential for the Fe(III)/Fe(II) reaction. This signal is assigned to transfer of the radical electron because the electron tends to be removed from the macrocyclic system. In other words, the Fe⁴⁺ ion form of compound **3-Fe** is more stable than the possible Fe³⁺ radical form under the current electrochemical conditions, which further demonstrates the importance of heme distortion in forming and stabilizing high-valence iron(IV) species.

The formation and stability of each new tautomer of the Fe³⁺ ion are energetically unfavorable. An energy ladder model and the corresponding fractional et model developed in this work clearly explain the pivotal role of core size in tautomer formation and stability. Formation of high-valence Fe⁴⁺ is an important subject that has puzzled scientists in the bioinorganic field for decades;^{60,61} this energy ladder model may afford a valuable reference for this subject.

Conclusions

In conclusion, the structure of the Fe³⁺ ions in macrocycles can undergo finer splitting besides simple conversion of spin modes under strong core contraction. This behavior was confirmed through detailed analysis of the crystal structures, and spectral and electrochemical properties of a series of strapped iron porphyrins. The possibility of four d electron tautomers of the Fe³⁺ ion are directly supported by these results, and their formation can be rationalized by considering an energy ladder

model. The large energy gap that stabilizes highly reactive Fe⁴⁺ may be overcome through a fractional et pathway with the aid of a gradient effect of energy levels. This fractional et allows unstable Fe⁴⁺ species to be formed and stabilized in porphyrins. These findings deepen our understanding of the changes of electronic structure in metallic ions during core contraction, and explain why heme needs macrocyclic distortion and how this distortion works, as well as providing a novel avenue to simulate the unique biochemical functions of economic metals like Fe and Co.

Acknowledgements

This work was supported by the National Natural Science Foundation of China (No: 21372069, and 21071051). Prof. Jianxiu Wang of Central South University is also acknowledged for his valuable help.

Notes and references

^a School of Chemistry and Chemical Engineering, Key Laboratory of 'Theoretical Organic Chemistry and Function Molecule' of the Ministry of Education, Hunan University of Science and Technology, Xiangtan 411201, China.

* E-mail: zhouzaichun@hnust.edu.cn

Electronic Supplementary Information (ESI) available: Discussion about the crystal structures and structural parameters of model compounds. See DOI: 10.1039/b000000x/

- 1 W. Nam, *Acc. Chem. Res.* 2007, **40**, 522–531.
- 2 Z. Pan, Q. Wang, X. Sheng, J. H. Horner and M. Newcomb, *J. Am. Chem. Soc.* 2009, **131**, 2621–2628.
- 3 J. T. Groves and Y. Z. Han, (1995) in *Cytochrome P450: Structure, Mechanism and Biochemistry* (P. R. Ortiz de Montellano, Ed.) Chapter 1, pp 3–48, Plenum, New York.
- 4 B. Meunier, S. P. de Visser,; S. Shaik, *Chem. Rev.* 2004, **104**, 3947–3980.
- 5 P. R. Ortiz de Montellano and J. De Voss, *Nat. Prod. Rep.* 2002, **19**, 477–493.

- 6 R. K. Behan, L. M. Hoffart, K. L. Stone, C. Krebs, and M. T. Green, Evidence for Basic Ferryls in Cytochromes P450, *J. Am. Chem. Soc.*, 2006, **128** (35), 11471–11474.
- 7 W. A. Lee, T. S. Calderwood, and T. C. Bruice, *Proc. Natl. Acad. Sci. U. S. A.* 1985, **82**, 4301–4305.
- 8 G. J. Abhilash, J. Bhuyan, P. Singh, S. Maji, K. Pal and S. Sarkar, *Inorg. Chem.*, 2009, **48**, 1790–1792.
- 9 J. T. Groves, R. C. Haushalter, M. Nakamura, T. E. Nemo and B. J. Evans, *J. Am. Chem. Soc.* 1981, **103**, 2884–2886.
- 10 L. M. Jensen, Y. T. Meharena, V. L. Davidson, T. L. Poulos, B. Hedman, C. M. Wilmot and R. Sarangi, *J. Biol. Inorg. Chem.* 2012, **17**, 1241–1255.
- 11 P. Pellicena, D. S. Karow, E. M. Boon, M. A. Marletta and J. Kuriyan, *Proc. Natl. Acad. Sci. U.S.A.* 2004, **101**, 12854–12859.
- 12 J.-C. Rain, L. Selig, H. De Reuse, V. Battaglia, C. Reverdy, S. Simon, G. Lenzen, F. Petel, J. Wojcik, V. Schächter, Y. Chemama, A. Labigne and P. Legrain, *Nature* 2001, **409**, 211–215.
- 13 J. A. Kovacs, *Science* 2003, **299**, 1024–1025.
- 14 Y. Sun, A. Benabbas, W. Zeng, J. G. Kleingardner, K. L. Bren and P. M. Champion, *Proc. Natl. Acad. Sci. USA* 2014, **111**, 6570–6575.
- 15 J. Pang, X. Li, K. Morokuma, N. S. Scrutton and M. J. Sutcliffe, *J. Am. Chem. Soc.* 2012, **134**, 2367–2377.
- 16 S. Severance and I. Hamza, *Chem. Rev.* 2009, **109**, 4596–4616.
- 17 E. M. Maes, S. A. Roberts, A. Weichsel and W. R. Montfort, *Biochemistry* 2005, **44**, 12690–12699.
- 18 T. Shokhireva, R. E. Berry, E. Uno, C. A. Balfour, H. Zhang and F. A. Walker, *Proc. Natl. Acad. Sci. U.S.A.* 2003, **100**, 3778–3783.
- 19 Z. C. Zhou, C. Z. Cao, Q. H. Liu and R. Q. Jiang, *Org. Lett.*, 2010, **12**, 1780–1783.
- 20 Z. C. Zhou, X. Zhang, Q. H. Liu, Z. Q. Yan, C. J. Lv and G. Long, *Inorg. Chem.* 2013, **52**, 10258–10263.
- 21 D. Li, D. J. Stuehr, S. R. Yeh and D. L. Rousseau, *J. Biol. Chem.* 2004, **279**, 26489–26499.
- 22 L. M. R. Jensen, R. Sanishvili, V. L. Davidson and C. M. Wilmot, *Science*, 2010, **327**, 1392–1394.
- 23 Z. C. Zhou, M. Shen, C. Z. Cao, Q. H. Liu and Z. Q. Yan, *Chem. Eur. J.* 2012, **18**, 7675–7679.
- 24 Z. C. Zhou, Q. H. Liu, Z. Q. Yan, G. Long, X. Zhang, C. Z. Cao and R. Q. Jiang, *Org. Lett.* 2013, **15**, 606–609.
- 25 The effect of core-size control by macrocyclic distortion on electronic structure is similar for Co and Fe ions.
- 26 (a) M. Nakamura, *Coord. Chem. Rev.* 2006, **250**, 2271–2294. (b) T. Sakai, Y. Ohgo, T. Ikeue, M. Takahashi, M. Takeda and M. Nakamura, *J. Am. Chem. Soc.* 2003, **125**, 13028–13029.
- 27 (a) H. Duval, V. Bulach, J. Fischer and R. Weiss, *Inorg. Chem.*, 1999, **38**, 5495–5501. (b) M. W. Renner, K. M. Barkigia, D. Melamed, J.-P. Gisselbrecht, N. Y. Nelson, K. M. Smith and J. Fajer, *Res. Chem. Intermed.*, 2002, **28**, 741–759.
- 28 C. Olea, Jr., E. M. Boon, P. Pellicena, J. Kuriyan and M. A. Marletta, *ACS Chem. Biol.* 2008, **3**, 703–710.
- 29 M. Newcomb, R. Zhang, R. E. P. Chandrasena, J. A. Halgrimson, J. H. Horner, T. M. Makris and S. G. Sligar, *J. Am. Chem. Soc.* 2006, **128**, 4580–4581.
- 30 T. Toraya, *Chem. Rev.*, 2003, **103**, 2095–2128.
- 31 K. M. Kadish, J. Shao, Z. Ou, C. P. Gros, F. Bolze, J.-M. Barbe and R. Guilard, *Inorg. Chem.* 2003, **42**, 4062–4070.
- 32 J. A. Shelnutt, X. Z. Song, J. G. Ma, S. L. Jia, W. Jentzen and C. J. Medforth, *Chem. Soc. Rev.* 1998, **27**, 31–41.
- 33 R. D. Shannon, *Acta Cryst. A*, 1976, **32**, 751–767.
- 34 W. M. Haynes, *Handbook of Chemistry and Physics*, 91st ed. CRC Press: Boca Raton, FL, 2010 section 9, p 18, and section 12, p 11.
- 35 S. P. Rath, M. M. Olmstead, and A. L. Balch, *J. Am. Chem. Soc.*, 2004, **126**, 6379–6386.
- 36 K. C. Christoforidis, M. Louloui, E. R. Milaeva and Y. Deligiannakis, *J. Catal.*, 2010, **270**, 153–162.
- 37 X. Li, R. Fu, S. Lee, C. Krebs, V. L. Davidson and A. Liu, *Proc Natl Acad Sci USA*. 2008, **105**, 8597–8600.
- 38 T. Picaud, C. Le Moigne, B. Looock, M. Mometeau and A. Desbois, *J. Am. Chem. Soc.* 2003, **125**, 11616–11625.
- 39 R. J. Deeth, *J. Am. Chem. Soc.*, 1999, **121**, 6074–6075.
- 40 R. J. Deeth and N. Fey, *J. Comput. Chem.*, 2004, **25**, 1840–1848.
- 41 R. Patra, D. Sahoo, S. Dey, D. Sil, and S. P. Rath, *Inorg. Chem.*, 2012, **51**, 11294–11305.

- 42 S. P. de Visser, F. Ogliaro, Z. Gross and S. Shaik, *Chem. Eur. J.*, 2001, **7**, 4954–4960.
- 43 S. P. deVisser, S. Shaik, P. K. Sharma, D. Kumar, and W. Thiel, *J. Am. Chem. Soc.*, 2003, **125**, 15779–15788.
- 44 L. A. Yatsunyk, M. D. Carducci, and F. A. Walker, *J. Am. Chem. Soc.* 2003, **125**, 15986–16005.
- 45 A. P. Weber, A. N. Caruso, E. Vescovo, M. E. Ali, K. Tarafder, S. Z. Janjua, J. T. Sadowski and P. M. Oppeneer, *Phys. Rev.B*, 2013, **87**, 18441-1–18441-8.
- 46 H. Ogura, L. Yatsunyk, C. J. Medforth, K. M. Smith, K. M. Barkigia, M. W. Renner, D. Melamed, F. A. Walker, *J. Am. Chem. Soc.* 2001, **123**, 6564-6578.
- 47 R. Patra, A. Chaudhary, S. Kumar G. and S. P. Rath, *Inorg. Chem.*, 2010, **49**, 2057–2067.
- 48 T. Sakai, Y. Ohgo, T. Ikeue, M. Takahashi, M. Takeda and M. Nakamura, *J. Am. Chem. Soc.*, 2003, **125**, 13028–13029.
- 49 T. Ikeue, Y. Ohgo, T. Yamaguchi, M. Takahashi, M. Takeda and M. Nakamura, *Angew. Chem., Int. Ed.* 2001, **40**, 2617–2620.
- 50 Y. M. Goh and W. Nam, *Inorg. Chem.*, 1999, **38**, 914–920.
- 51 N. Abu Tarboush, L. M. R. Jensen, M. L. Feng, H. Tachikawa, C. M. Wilmot and V. L. Davidson, *Biochemistry*, 2010, **49**, 9783–9791.
- 52 I. Barr, A. T. Smith, R. Senturia, Y. Q. Chen, B. D. Scheidemantle, J. N. Burstyn and F. Guo, *J. Biol. Chem.* 2011, **286**, 16716–16725.
- 53 K. M. Kadish, E. Van Caemelbecke, F. D'Souza, C. J. Medforth, K. M. Smith, A. Tabard and R. Guillard, *Inorg. Chem.* 1995, **34**, 2984–2989.
- 54 S. Maree and T. Nyokong, *J. Electroanal. Chem.*, 2000, **492**, 120–127.
- 55 J. Metz, O. Schneider and M. Hanack, *Inorg. Chem.*, 1984, **23**, 1065–1071.
- 56 Y. Fang, M. O. Senge, E. Van Caemelbecke, K. M. Smith, C. J. Medforth, M. Zhang and K. M. Kadish, *Inorg. Chem.* 2014, **53**, 10772–10778.
- 57 J. A. Hodge, M. G. Hill and H. B. Gray, *Inorg. Chem.*, 1995, **34**, 809–812.
- 58 K. M. Kadish, B. Boisselier-Cocolios, B. Simonet, D. Chang, H. Ledon and P. Cocolios, *Inorg. Chem.* 1985, **24**, 2148–2156.
- 59 C. Swistak and K. M. Kadish, *Inorg. Chem.* 1987, **26**, 405–412.
- 60 D. Schröder, S. Shaik and H. Schwarz, *Acc. Chem. Res.* 2000, **33**, 139–145.
- 61 W. A., Herrmann, *Angew. Chem. Int. Ed.* 2002, **41**, 1290–1309. *Angew. Chem.*, 2002, **114**, 1342–1363.